9

Carbon Nanotubes and Nanowires for Biological Sensing

Jun Li, Hou Tee Ng, and Hua Chen

Summary

This chapter reviews the recent development in biological sensing using nanotechnologies based on carbon nanotubes and various nanowires. These 1D materials have shown unique properties that are efficient in interacting with biomolecules of similar dimensions, i.e., on a nanometer scale. Various aspects including synthesis, materials properties, device fabrication, biofunctionalization, and biological sensing applications of such materials are reviewed. The potential of such integrated nanobiosensors in providing ultrahigh sensitivity, fast response, and high-degree multiplex detection, yet with minimum sample requirements is demonstrated. This chapter is intended to provide comprehensive updated information for people from a variety of backgrounds but with common interests in the fast-moving interdisciplinary field of nanobiotechnology.

Key Words: Carbon nanotube; single-walled carbon nanotube; multiwalled carbon nanotube; nanowires; chemical vapor deposition; lithography; self-assembly; scanning probe microscopy; field-effect-transistor; nanoelectronics.

1. Introduction

Efficient biological sensing requires directly interrogating individual biomolecules with a physical dimension of about 1 to 100 nm. Development in this field strongly demands techniques and probing tools extending to similar length scales. This has been one of the major driving forces for nanotechnology in recent years. As the size of the materials is reduced to the nanometer regime, they show many new electronic, optical, and mechanical properties, which are more directly associated with the environment and target samples. Although the majority of raw nanomaterials are nanoparticles, high-aspect ratio one-dimensional (1D) materials such as carbon nanotubes (CNTs) and various nanowires (NWs) are more attractive as building blocks in the fabrication of

From: *Methods in Molecular Biology, vol. 300:*
Protein Nanotechnology, Protocols, Instrumentation, and Applications
Edited by: T. Vo-Dinh © Humana Press Inc., Totowa, NJ

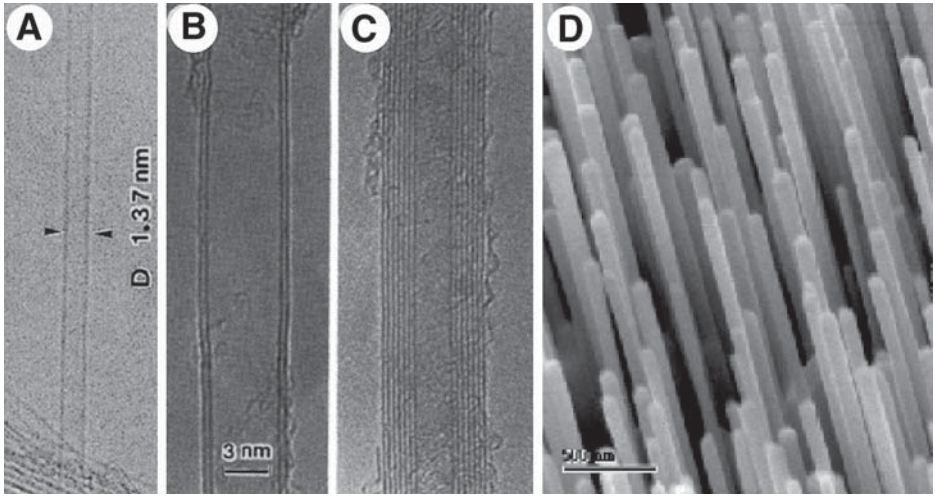

Fig. 1. Transmission electron microscopy (TEM) images of **(A)** a SWCNT and **(B,C)** two types of MWCNTs, and **(D)** scanning electron microscopy (SEM) image of an array of ZnO NWs. (Panel [A] is reprinted from **ref.** ***10*** with permission and panels [B] and [C] are reprinted from **ref.** ***9*** with permission. Copyright 1991 and 1993, respectively, Nature Publishing Group, http://www.nature.com.)

devices. The potential of CNTs and NWs as sensing elements and tools for biological applications as well as for detecting gases and small chemicals has been recently recognized. Promising results in improving sensitivity, lowering detection limit, reducing sample amount, and increasing the degree of multiplex and miniaturization have been reported based on CNTs ***(1,2)*** and NWs ***(3,4)***. Even though these studies are still in early research stages, they have shown great potential for future biotechnologies. This chapter summarizes, from a technology development point of view, the recent progress in the development of biological sensors using CNTs and NWs, it is our hope to attract interest in exploring the potential applications of such technologies in biomedical research.

CNTs belong to a family of materials consisting of seamless graphitic cylinders with extremely high aspect ratios ***(5–8)***. The typical diameter varies from about 1 nm to hundreds of nanometers, and the length spans from tens of nanometers to hundreds of microns or even centimeters. Scientists in NEC Corporation originally discovered the cylindrical structure of CNTs in 1991 ***(9)***. A CNT may consist of one graphitic layer, referred to as single-walled CNTs (SWCNTs) ***(10)***, as shown in **Fig. 1A**, or multi graphitic layers, referred to as multiwalled CNTs (MWCNTs) ***(9)***, as shown in **Fig. 1B,C**. SWCNTs normally give a smaller diameter (down to 7 Å) and show electronics properties strongly

dependent on the helicity, namely the (*m*,*n*) lattice vector in the graphitic sheet along which it is rolled into a tube ***(11)***. It is known that SWCNTs are semiconducting if their chirality (*m*,*n*) satisfies $m - n \neq 3 \times$ integer ***(5–8)***. MWCNTs consist of a random mixture of all possible helicities in each shell ***(12)***.

Owing to the intriguing nanometer-scale structures and unique properties, CNTs have quickly attracted intensive attention in the past few years in many fields such as nanoelectronic devices ***(12–20)***, composite materials ***(21)***, field-emission devices ***(22,23)***, atomic force microscope probes ***(24–27)***, and hydrogen/lithium ion storage ***(28,29)***. Many studies reported potential for ultrahigh sensitivity sensors as well ***(1,20,30–32)***. The extremely high surface-to-volume ratio of CNTs is ideal for efficient adsorption. The (1D) quantum wire nature makes their electronic properties extremely sensitive to gas or chemical adsorption. Both of these factors are essential for high-sensitivity sensors. In the past few years, CNT sensors have been demonstrated in many applications involving gas molecules, liquid-phase chemicals, and biomolecules, showing improved performance compared with conventional sensors utilizing micro- or macromaterials and thin films ***(2)***. Depending on applications, sensing devices can be fabricated using single free-standing CNTs ***(25,26)***, semiconducting SWCNT field-effect-transistors (FETs) ***(1,20,33,34)***, well-defined nanoelectrode arrays ***(35)***, or porous films ***(32,36,37)***.

NWs, on the other hand, typically refer to highly crystalline, wirelike 1D materials consisting of metals ***(38)***, semiconductors ***(3,39)***, or inorganic compounds ***(4,40)***. They can be synthesized with a high aspect ratio similar to that of CNTs, i.e., about a few to hundreds of nanometers in diameter and more than microns in length. **Figure 1D** shows a well-aligned array of ZnO NWs with an average diameter of approx 100 nm and length more than microns. Besides showing similar properties, such as high aspect ratio and large surface-to-volume ratio, CNTs, NWs have well-defined crystalline structure. The broad choice of various crystalline materials and doping methods makes the electronic and optical properties of NWs tunable with a high degree of freedom and precision. With the development of new synthesis methods, NWs have attracted more and more attention for sensor applications.

Another category of NWs is based on templating methods. These materials are the assembly of intrinsically heterogeneous biological and solid-state nanomaterial components instead of homogeneous structures. The nano-/bio-assembly NWs consist of two approaches: (1) CNTs or crystalline NWs serving as templates on which biomolecules aggregate into nanoscale wirelike structures ***(41)***, and (2) DNA or protein macromolecular backbones or assembly serving as templates on which nanoparticles are deposited to form nanoscale wirelike structures ***(42)***. Both of these approaches have been demonstrated in heterogeneously integrated nano-biosystems for biological sens-

ing, which combine the biorecognition-driven self-assembly functionalities with desired solid-state electronics properties.

2. Growth of Materials and Device Fabrication

2.1. Growth of CNTs

Finding the solutions to grow CNTs with desired quantities and qualities is an active, ongoing research topic. A host of experimental approaches have been explored, improved, and modified to successfully synthesize CNTs, both single- and multiwalled, for sensor applications. The typical techniques used include electrical arc discharge, laser ablation, and chemical vapor deposition. In most growth processes, a catalyst that is either a metal or a mixed alloy is used.

Iijima and Ichihashi ***(10)*** and Bethune et al. ***(43)*** first demonstrated the growth of SWCNTs, though in small quantities, by using the electrical arc-discharge techniques. The SWCNTs were typically accompanied by a substantial amount of amorphous carbon, carbon nanoparticles, and other carbon-based materials. By using the laser ablation method, Thess et al. ***(44)*** further improved the purity and synthesized SWCNTs on the grams quantity. The as-synthesized SWCNTs present mostly in the form of ropes with individual nanotubes aggregating into hexagonal crystals owing to the van der Waals interaction. Subsequent studies by other groups have improved on either the designs or experimental formulations to obtain better quality and larger quantity products. For example, Kajiura et al. ***(45)*** used a newly designed chamber that was equipped with a filtering zone to produce a high content of SWCNT ropes under controlled gas flow conditions. Journet et al. ***(46)*** optimized the growth of SWCNTs by incorporating yttrium and nickel into a carbon anode. Both of these techniques have also been successfully used to synthesize MWCNTs.

Recently, chemical vapor deposition (CVD) has gained popularity in synthesizing both SWCNTs and MWCNTs with good yields and particularly for direct growth device fabrication. A typical growth process involves passing a hydrocarbon gas over a heated catalyst at high temperature for a period of time. Kong et al. ***(47)*** demonstrated using the techniques to synthesize SWCNTs with high quality by passing methane over alumina-supported catalyst in a temperature range of 850 to 1000°C. By optimizing the catalyst preparation and growth conditions, the quality and yields of the nanotubes could be further improved as demonstrated by many studies ***(48–51)***. More recently, Bronikowski et al. ***(52)*** demonstrated large-scale production (10 g/d) of high-purity SWCNTs using a gas-phase CVD process, termed HiPco process. SWCNT material of up to 97 mol% purity could be produced at a rate of 450 mg/h.

Plasma enhanced CVD (PECVD), with the advantage of compatibility with semiconductor processes, has attracted extensive attention in the growth of CNTs for device fabrication ***(53–55)***. A single or an array of CNTs can be grown at sites precisely defined by lithographic techniques down to tens of nanometers ***(55)***. The alignment can also be precisely controlled by an electrical field. The only drawback is that the CNTs grown by PECVD are more defective, with the graphitic layer not perfectly parallel to the tube axis. Many bamboo-like close shells are formed along the tube instead of forming perfect hollow channels running from one end all the way to the other end. However, such defective structures were found not critical for many sensor applications ***(35)***. With continual effort in the development of growth techniques and methodology, it is expected that CNTs with the desired properties, qualities, and quantities will be obtained in the near future.

2.2. Growth of Crystalline NWs

Crystalline 1D NWs can be formed with metals, semiconductors, or inorganic compounds. They have shown potential in a wide range of applications including nanoelectronics, nanosensors, and nanobiotechnology. Different synthetic strategies have been developed for obtaining desired 1D NWs, which can be divided into two categories using wet chemical methods and vapor-phase methods, respectively.

In the growth of 1D nanowires dictated by the anisotropic crystallographic nature of the material, Stejny et al. ***(56)*** demonstrated that inorganic NWs of poly(sulfur nitride) having a diameter of approx 20 nm and a length of hundreds of micrometers could be synthesized by taking advantage of their highly anisotropic structural bonding. Using a similar strategy, Golden et al. ***(57)*** and Venkataraman and Lieber ***(58)*** showed the synthesis of $(Mo_3Se_3^-)_n$ and molybdenum selenide molecular wires, respectively. Making use of the hexagonally packed helical chains of Se atoms along their *c*-axis, Gates et al. ***(59)*** demonstrated that a generic, solution-phase approach could be used for the large-scale synthesis of uniform NWs of t-Se.

Another strategy involves using a template to assist in the synthesis of 1D NWs. The template serves as a scaffold within (or around) which a desired material could be *in situ* generated with its morphology complementary to that of the template. For example, Limmer et al. ***(60)*** showed the growth of uniform arrays of NWs of Pb(Zr, Ti)O_3 in porous alumina membranes. Although the synthesized NWs are typically polycrystalline, single crystalline NWs could be obtained with careful selection of the growth conditions. Barbic et al. ***(61)*** and Molares et al. ***(62)*** demonstrated growth of single crystalline silver and copper NWs, respectively, using electrodeless and pulse electrodeposition methods. Using a different templating platform, Müller et al. ***(63)*** showed that

it is possible to fabricate large arrays of Ge NWs by templating against the V-grooves etched into the surfaces of Si(100) substrates. Sugawara et al. ***(64)*** further demonstrated that three-dimensional (3D) arrays of iron NWs could be obtained by templating against relief features existing on the surfaces of NaCl crystals. Other templating schemes involving forming self-assembled molecular structures against existing nanostructures have also been successfully used to obtain a variety of NWs ***(65)***.

Vapor-phase synthesis, on the other hand, is probably the most extensively explored method for the fabrication of 1D NWs. By maintaining a low supersaturation level and vapor pressure, 1D nanostructures could, in principle, be synthesized from their bulk materials. A main advantage of the vapor-phase method lies in its simplicity and accessibility. In a typical growth process, the vapor species are first formed by evaporation, followed by chemical reduction, transportation, and condensation of gas species onto suitable substrates. In the direct vapor-phase method, Zhang et al. ***(66)*** showed successful growth of Si_3N_4, SiC, Ga_2O_3, and ZnO NWs by heating the powders of these materials at elevated temperatures. Using an indirect vapor-phase method, Yang and Lieber ***(67)*** showed the growth of MgO NWs using a carbothermal reduction process. Recently, Shi et al. ***(68)*** observed the growth of Si NWs by using a mixture of Si and SiO_2 in the feedstocks. Laser ablation was used to assist in the vaporization of these bulk materials.

Among the various vapor-based methods, a growth process involving a vapor-liquid-solid (VLS) mechanism is poised to be the most successful approach for generating NWs with single crystalline structures. Numerous groups have synthesized a variety of NWs from their respective inorganic materials ***(69–73)***. A critical component of the VLS mechanistic growth approach involves dissolution of the gaseous reactants into a liquid catalytic nanoparticle, which acts as a soft template for the nucleation and growth of 1D NWs.

A major challenge in the synthesis of 1D NWs is how to tailor their diameter, length, and properties uniformly in a single growth process. This is particularly important in many practical applications that require high homogeneity in their structural, physical, and electronic properties.

2.3. Nanobiosensing Devices

Figure 2 summarizes four types of the most commonly used biological sensing devices based on CNTs and NWs, which covers most studies reported in the literature by now. Depending on the sensing applications, different device architectures and fabrication routes are required to achieve successfully their desired functions. Common to all, CNTs or NWs are critical components of the sensing devices, which are integrated either directly or indirectly during the fabrication routes. A variety of methods, ranging from advanced micro- or

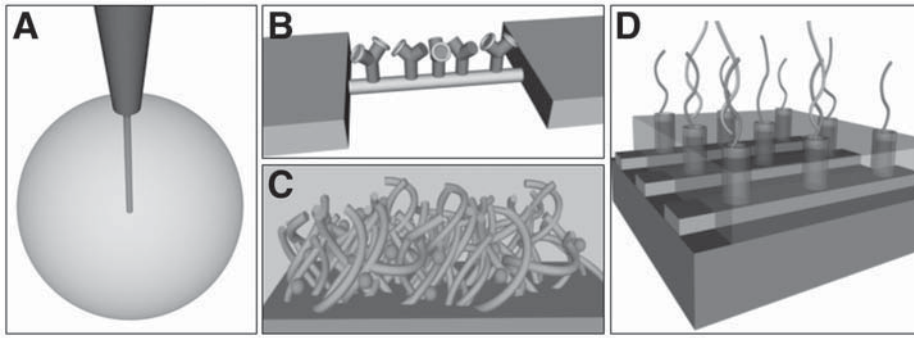

Fig. 2. Schematic of four types of CNT/NW devices for biological sensing: **(A)** single CNT or NW extended from a microtip to probe a single cell or single molecules; **(B)** FET device using a single semiconducting CNT or NW; **(C)** porous CNT/NW film as electrochemical biosensor; **(D)** nanoelectrode array-based electrochemical biosensor.

nanolithographic techniques to handmade processes, have been demonstrated by various researchers to build functional devices. Generally, CNTs/NWs could be the sensing elements whose properties are changed on occurrence of the biological events' or the transducers that transfer the changed signal to the measuring units. The sensing device could use a single CNT/NW or an ensemble of such materials.

The most straightforward biological sensing employs a single CNT or NW to probe the biochemical environment in a single living cell or interrogate a single biomolecule (as shown in **Fig. 2A**). The CNT/NW probe can be attached to the pulled tip of an optical fiber for optical detection ***(74)*** or an electrode for electrical or electrochemical measurements ***(75)***. Normally, for such applications, the sidewalls of the nanoprobe have to be shielded or insulated to reduce the background so that the small signal from the very end of the probe can be detected. The CNT/NW probes provide the best spatial resolution as well as ultrahigh sensitivity and short response time. The small size, high aspect ratio, and mechanical robustness of CNTs were also employed as the physical probe for high-resolution scanning probe microscopy (SPM). This technique is powerful for illustrating the structure of single molecules such as DNA and proteins with the resolution down to a few nanometers.

A semiconducting CNT or NW can be used to construct a FET, as shown in **Fig. 2B**, using nanolithographic techniques. Such a device consists of a semiconducting CNT or NW connected to two contact electrodes (source and drain) on an oxide-covered Si substrate that could serve as the gate electrode ***(1,13)***. Conventional FETs fabricated with semiconductors such as Si have been

configured as sensors by modifying the gate oxide (without the gate electrode) with molecular receptors or ion-selective membranes for the analytes of interest ***(76)***. The binding or adsorption of charged species could produce an electric field that depletes or accumulates carriers within the semiconducting material similar to the gate potential. As a result, the conductance between the source and drain electrodes is dramatically changed. Chemical sensors based on such a mechanism referred to as chemical field-effect-transistors ***(76)*** have been used for many applications since the 1980's.

As we mentioned in the Introduction, SWCNTs have well-defined structures. The helicity of the SWCNT determines whether it is metallic or semiconducting. It has been demonstrated that a semiconducting SWCNT (S-SWCNT) FET exhibits p-type transistor characteristics with the conductance tunable over several orders of magnitude by changing the gate voltage applied on the Si substrate ***(1)***. Such a phenomenon was attributed to the adsorption of O_2 as the electron acceptor in an ambient environment. Since every carbon atom is exposed at the surface, SWCNTs are highly efficient for gas adsorption. In addition, a theoretical work predicts about 0.1 electron transfers per O_2 molecule ***(77)***. Owing to the small size, this gives a big carrier density in the "bulk" SWCNT that would dramatically change the electronic behavior of the FET. The quantum wire nature of the SWCNT makes the conductance of the tube even more sensitive because any partial point charge could completely deplete the local carrier along the 1D wire. Therefore, the sensitivity of single-molecule adsorption/desorption could, in principle, be achieved with such miniaturized S-SWCNT FETs. Semiconducting NWs (S-NWs) such as Si ***(3)*** and In_2O_3 ***(4)*** have also been recently demonstrated in FET sensing devices. The applications of such devices in biological sensing are discussed in **Subheading 3.2.**

The large surface-to-volume ratio and good electrical conductance along the tube axis make CNTs attractive for enzyme-based electrochemical sensors. CNTs can be cast as a thin film on conventional electrodes ***(78–80)*** or used as a 3D porous film ***(32,36,37)*** (as shown in **Fig. 2C**). Such crude CNT ensembles serve both as large immobilization matrices and as mediators to improve the electron-transfer between the enzyme-active site and the electrochemical transducer. Improved electrochemical behavior of NADH ***(80)***, neurotransmitters ***(32)***, and enzymes ***(79)*** has been reported.

The last type of CNT/NW device is also an electrochemical sensor based on an array of vertically aligned CNTs embedded in SiO_2 matrices, as schematically shown in **Fig. 2D**. The electrochemical signal is characteristic of the reduction/oxidation (redox) reaction of the analytes instead of nonspecific charges sensed by FETs, resulting in very good specificity comparable to fluorescence-based optical techniques that are commonly used in today's biology research. In addition, a high degree of miniaturization and multiplex detection

can be realized for molecular diagnosis using individually addressed microelectrode array integrated with microelectronics and microfluidics systems ***(81–84)***, which is more attractive than optical techniques, particularly for quick and simple diagnostics. However, the sensitivity of electrochemical techniques using traditional macro- and microelectrodes is orders of magnitude lower than those of optical techniques, which limits their use in many applications. Nanoscale sensing elements have been actively pursued to seek solutions for improving the sensitivity of electrochemical techniques.

The performance of electrodes with respect to speed and spatial resolution is known to scale inversely with the electrode radius ***(85–87)***. It is of interest for biosensing to reduce the radius of electrodes to 10–100 nm, approaching the size of biomolecules. Li et al. ***(35)*** demonstrated that nanoelectrodes, particularly a MWCNT-based nanoelectrode array, with an average diameter of 30 to 100 nm, can be integrated into an electrochemical system for ultrasensitive chemical and DNA detection. The nanoelectrode array is fabricated with a bottom-up scheme resulting in a precisely positioned and well-aligned MWCNT array embedded in a planarized SiO_2 matrix ***(55,88)***. The vertically aligned MWCNTs were first grown using direct current (DC)–biased hot-filament plasma CVD on a metal film–covered silicon substrate. They were then subjected to tetraethyloxysilicate CVD for gap filling of SiO_2. SiO_2 dielectrics was found to fill conformally in the gap between individual MWCNTs and hence reinforced the MWCNT array. Excess SiO_2 was subsequently removed, allowing exposure of the MWCNT tips via a mechanical polishing step. The open ends of MWCNTs exposed at the dielectric surface act as nanoelectrodes. **Figure 3** shows SEM images of a CNT array grown on multiplex microelectrodes with different densities defined by lithographic techniques. The surface of an encapsulated and planarized array shows only the very end of CNTs exposed as well-defined nanoelectrodes. Such a nanoelectrode array showed characteristic electrochemical behavior for redox species both in bulk solution and immobilized at the CNT ends. Dramatic improvements in sensitivity and time constant were observed ***(35)***.

CNTs have demonstrated many advantages in nanoelectrode applications. The wide electropotential window, flexible surface chemistry, and biocompatibility make the MWCNT array an attractive electrode similar to other widely used carbon electrodes. The open end of an MWNT is expected to show a fast electron transfer rate (ETR) similar to that of the graphite edge-plane electrode, whereas the sidewall is inert like the graphite basal plane ***(89)***. Fast ETR is demonstrated along the tube axis ***(75,90)***. Such an MWCNT electrode could interrogate target species, down to the single-molecule level, at one end and sustain electron transport along the tube axis to the measuring circuit with minimum interference from the environment. Whereas a single

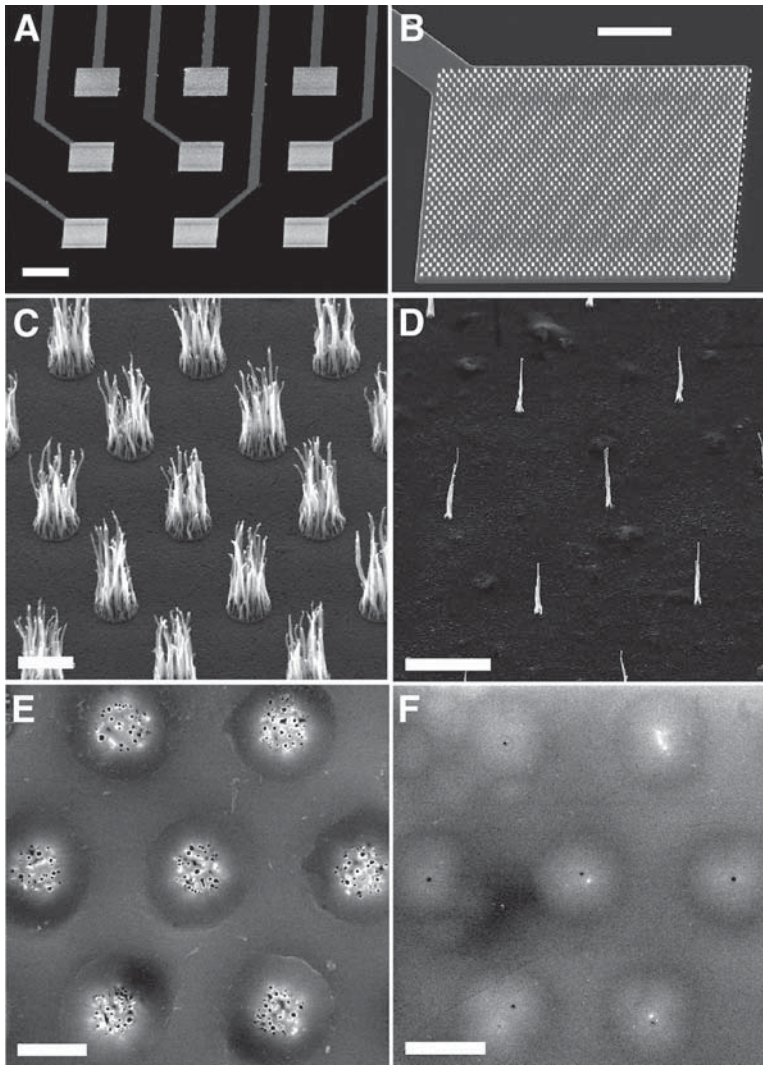

Fig. 3. SEM images of **(A)** 3 × 3 electrode array; **(B)** array of MWCNT bundles on one of the microelectrode pads; **(C,D)** array of MWCNTs at UV-lithography– and e-beam–patterned Ni spots, respectively; **(E,F)** surface of polished MWCNT array electrodes grown on 2-μm and 100-nm spots, respectively. Panels (A–D) are 45° perspective views and panels (E) and (F) are top views. Bars = 200, 50, 2, 5, 2, and 2 μm, respectively.

nanoelectrode can provide the desired temporal and spatial advantages, the nanoelectrode array serves the needs for analytical applications requiring reliable statistics and multiplex detection.

2.4. Functionalization of CNTs/NWs for Biological Sensing

A common feature for biological sensing is the requirement of immobilization of biomolecules with specific functionalities to the sensing device. These biomolecules serve as probes either to specifically bind particular species in the testing sample or to specifically catalyze the reaction of the analyte. Such an event produces a change in chemical or physical properties that can be converted into a measurable signal by the transducer. The specific recognition of the target molecules is the essential feature for biological sensing. The common probe and target (analyte) recognition mechanisms include (1) antibody–antigen interactions, (2) nucleic acid hybridizations, (3) enzymatic reactions, and (4) cellular interactions. Depending on the device and its sensing mechanism, different functionalization methods have to be adapted. We can separate the functionalization methods into three categories to cover all the biological sensing methods that are summarized in the next section. These are (1) covalent binding to the open ends of CNTs, (2) noncovalent binding to the sidewall of CNTs, and (3) covalent binding to NWs.

CNTs, from a structural point of view, are quite similar to a roll of graphitic sheets. The sidewalls have very inert chemical properties similar to graphite basal planes. The open ends of CNTs, on the other hand, are similar to graphite edge planes, which are much more reactive owing to the dangling sp^2 bonds. For measuring the chemical force of single molecules or single-cell surfaces with CNT SPM tips and using CNT nanoelectrodes for biosensing ***(35)***, the open end of the CNTs needs to be functionalized. Lieber et al. ***(25,91)*** demonstrated that the open end of an SWCNT is rich with the –COOH group and thus can be used for selective covalent bonding of primary amine molecules through amide bonds facilitated by the coupling reagents *N*-hydroxysuccinimide' sometimes aided with dicyclohexylcarbodiimide. Williams et al. ***(92)*** used similar methods to functionalize the open end of an SWCNT with a peptide nucleic acid (PNA) with the sequence NH_2-Glu-GTGCTCATGGTG-$CONH_2$, in which Glu is a glutamate amino acid residue and the central block represents nucleic acid bases. A National Aeronautics and Space Administration (NASA) group demonstrated that primary amine–terminated DNA oligoprobes can be covalently functionalized to the open ends of an array of vertically aligned MWCNTs imbedded in SiO_2 matrix by a similar carbodiimide chemistry using the water-soluble coupling reagents 1-ethyl-3(3-dimethyl aminopropyl) carbodiimide hydrochloride and *N*-hydroxysulfo-succinimide ***(93)***.

For FET sensors, functionalization to the sidewall of CNTs is required ***(33,34,94,95)***. Because semiconducting SWNTs are used as the conducting channels whose electronic properties are monitored up on the binding of charged target molecules at the surface, the graphitic sp^2 sidewall structure has

to be preserved to maintain its inherit properties. Such a sidewall structure is strongly hydrophobic and chemically inert, which raises problems in biocompatibility and biofunctionalization for specific recognition. It has been reported that proteins such as streptavidin and HupR can adsorb strongly onto the MWCNT surface presumably via hydrophobic interactions between the aromatic CNT surface and hydrophobic domains of the proteins ***(41)***. A designed amphiphilic α-helical peptide has been found to spontaneously assemble onto the SWCNT surface in aqueous solution with the hydrophobic face of the helix noncovalently interacting with the CNT surface and the hydrophilic amino acid side chains extending outward from the exterior surface ***(96)***. Chen et al. ***(94)*** reported a noncovalent sidewall functionalization scheme whereby a variety of proteins were immobilized on SWCNTs functionalized by π-stacking of the conjugate pyrenyl group of 1-pyrenebutanoic acid succinimidyl ester. The succinimidyl ester group reacts with amine groups on lysine residues of proteins to form covalent amide linkages ***(94)***. However, all such noncovalent interaction–based immobilization methods lack specificity; in particular, the direct nonspecific binding of proteins to the CNTs needs to be suppressed for biological sensing. Extensive washing using conventional protocols was not sufficient to remove such nonspecifically bound proteins. For this purpose, a surfactant (Triton-X 100) was coadsorbed on the CNT surface with polyethylene glycol (PEG) ***(95)***. Such a coating was found to be effective in resisting nonspecific adsorption of streptavidin. Amine-terminated PEG can be used so that the biotin moiety can be added to the PEG chains through covalent linking with an amine-reactive biotin reagent, biotinamidocaproic acid 3-sulfo-*N*-hydroxysuccinimide ester ***(95)***. The functionalized CNTs have demonstrated specific recognition to streptavidin. A similar method using mixed polyethylene imine (PEI) and PEG coating was reported for functionalizing biotin to the sidewall of SWCNTs in FET devices ***(34)***. These methods can be extended to the recognition of other biomolecules based on specific interactions of antibody-antigen and complementary DNA strands.

Besides the application in FET sensing devices, the biofunctionalized CNTs also show much better solubility so that further chemistry or biochemistry can be applied. In addition, biorecognition can be employed to regulate the assembly of supramolecular structures, which may lead to new sensing devices. Since the integrity of the CNT structure is not as critical in such applications as in FETs, covalent sidewall functionalizations are also actively persued by the direct attachment of functional groups to the graphitic surface such as fluorination and hydrogenation or the use of carboxylic acids at the defect sites to form amide or ester linkages ***(97)***. Such sidewall functionalizations may particularly be applicable to MWCNT sensors in which CNTs only serve as the probe materials to transduce signals from the measured molecules and their own elec-

tronic properties are insensitive to the environment. For example, a MWCNT electrode functionalized with antibody or enzyme can be used as a single electrochemical probe to study biochemistry in a single cell ***(75)***. Sidewall functionalization of the MWCNT array can also greatly increase the enzyme (glucose oxidase) loading in the electrochemical glucose sensor ***(37)***. Some other studies on enzyme-based sensors using CNT-cast glassy carbon electrodes have demonstrated that even spontaneous adsorption or polymer wrapping can improve enzyme loading and electron transfer ***(78–80)***. From the biological side, peptides with selective affinity for CNTs were recently reported ***(98)***, which could lead to new methods for bio-nanointegration.

For metal NWs, such as Au, Ag, and Cu, strongly chemisorbed thiol molecules are commonly used as linkers for immobilizing biomolecules ***(99)***. Si or Ge NWs present a thin (approx 1 to 2 nm thick) native oxide film at the surface. Such NWs and other oxide NWs present abundant hydroxyl groups at the surface. Various silane molecules can be used as linkers to functionalize biomolecules ***(100,101)***. Polymer wrapping can also be applied to functionalize various NWs. Nonspecific adsorption could be used as well. Cui et al. ***(3)*** simply dipped Si NWs in biotinamidocaproyl-labeled bovine serum albumin followed by rinsing with phosphate buffer and demonstrated that specific binding with streptavidin target can be detected with a FET device down to at least a picomolar concentration range.

3. Applications and Mechanisms for Biological Sensing

3.1. Single-Cell/Single-Molecule Probes

The most direct application of CNTs/NWs for biological sensing is to use them as single probes, which gives great spatial resolution. With the small size, such probes can be inserted into a single cell for *in situ* measurements with minimum disturbance as well as ultrahigh sensitivity. Vo-Dinh et al. ***(74)*** demonstrated antibody-based nanobiosensors for the detection of benzo[*a*] pyrene tetrol (BPT), a biomarker for human exposure to the known carcinogen benzo[*a*] pyrene, by simply pulling an optical fiber to nanometer sizes at the tip. The distal end was covalently coated with anti-BPT antibodies through silane linkers. The nanobiosensors were inserted into individual cells, incubated for 5 min to allow antigen-antibody binding, and then removed for detection. The small size of the tips of these optical fiber nanosensors gives them several advantages over normal probes, including decreased response time and increased sensitivity. Such a nanobiosensor, based on fluorescence spectroscopy, shows a sensitivity down to approx 1.0×10^{-10} *M* for BPT ***(74,102)*** and an absolute limit of detection for BPT of approx 300 zeptomol (10^{-21} mol) ***(103)***.

With the recent development in CNTs and NWs, such wirelike nanomaterials can be adapted for similar techniques. In particular, ZnO NWs have been found

with nanolasing properties along the axial direction ***(40,104)***, which could be explored for optical-biomolecular detection. CNTs or metal NWs, on the other hand, can be used as nanoelectrodes ***(75)*** to measure the electrochemical reaction in a single cell or the reactivity of a single molecule. The electrical signal has the potential to reach single molecular sensitivity, by using a nanoelectrode ***(87)***.

Single CNTs attached to a scanning probe microscope tip have also attracted intensive interest owing to their small diameter, high aspect ratio, large Young's modulus, and mechanical robustness ***(24)***. They can be used as physical probes to obtain the highest resolution in studying the structure of macromolecules or cell surfaces. Li et al. ***(26)*** demonstrated the method for implementing and characterizing CNTs attached to a scanning probe microscope (SPM) tip for *in situ* imaging of DNA molecules on a mica surface within a buffer solution. They used a magnetically driven oscillating probe atomic force microscope with a silicon nitride cantilever (spring constant of $k = 0.1$) driven at a frequency of approximately kHz. A bundle of MWCNTs was attached to the pyramidal tip with an acrylic adhesive. The diameter of the bundles ranged from tens to hundreds of nanometers. Typically, a single MWCNT extended out and was used as a probe for SPM imaging. λ DNA molecules were spontaneously bound to the surface from 2 μg/mL solutions with the presence of approx 1 m*M* $MgCl_2$ for enhancing the DNA/mica interaction. **Figure 4** shows a SPM image of DNA molecules in a 2.3×2.3 μm^2 area. Single DNA molecules were clearly resolved. The resolution of DNA images is very uniform and consistent with the diameter of the CNT tip (approx 5 nm). SWCNT tips could provide even higher resolution ***(25,91)***. The double-helix structure of DNA may be resolved in the future by SPM techniques using SWCNT tips. The tip can also be functionalized to provide additional information about chemical force ***(25,91)***.

Woolley et al. ***(105)*** reported the direct haplotyping of kilobase-size DNA using SWCNT SPM probes. The haplotype of a subject—the specific alleles associated with each chromosome homolog—is a critical element in single-nucleotide polymorphism (SNP) mapping that leads to a greater comprehension of the genetic contribution to risk of common diseases such as cancer and heart disease. However, current methods for determining haplotypes have significant limitations that have prevented their use in large-scale genetic screening. For example, molecular techniques for determining haplotypes, such as allele-specific or single-molecule polymerase chain reaction (PCR) amplification, are hampered by the need to optimize stringent reaction conditions and the potential for significant error rates. Using SPM with high-resolution SWCNT probes, multiple polymorphic sites can be directly visualized by hybridizing specifically labeled oligonucleotides with the template DNA frag-

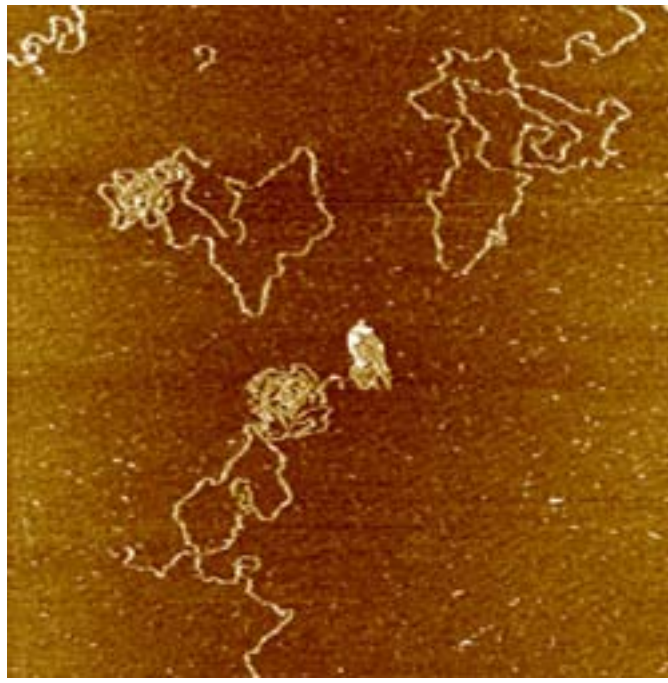

Fig. 4. SPM image of DNA molecules on 2.3 × 2.3 μm^2 mica surface submerged under 1 m*M* $MgCl_2$ buffer solution obtained with a single MWCNT tip.

ments of approx 100 to 10,000 bases. The positions of streptavidin and IRD800 labels at two sequences in M13mp18 were demonstrated. The SWCNT tips, with tip radii <3 nm and resolution of approx 10 base, made it possible for high-resolution multiplex detection to differentiate between labels such as streptavidin and the fluorophore IRD800 based on their size. This concept has been further applied to the determination of haplotypes on the UGT1A7 gene ***(105)***, which is under study for its role in cancer epidemiology. Direct haplotyping using SWCNT SPM probes represents a significant advance over conventional approaches and could facilitate the use of SNPs for association and linkage studies of inherited diseases and genetic risk ***(106)***.

The electronic properties of biomolecules such as DNAs have been extensively studied in the past few years owing to their potential for single molecular sensing. However, DNA molecules were found to be not very conductive even in the duplex form. There are also difficulties in assembling them into reliable devices. Williams et al. ***(92)*** reported on a study to couple SWCNTs covalently with PNA (an uncharged DNA analog). Hybridization of DNA fragments to the PNA sequence was measured with an atomic force microscope

under ambient conditions and indicated that the functionalization is specific to the open ends of SWCNTs with rare attachment to the sidewall. PNA was chosen owing to its chemical and biological stability. The uncharged PNA backbone gives rise to PNA-DNA duplexes that are more thermally stable than their DNA-DNA counterparts because there is no electrostatic repulsion. This method unites the unique properties of SWCNTs with the specific molecular recognition features of DNA, which may provide new means to incorporate SWCNTs into larger electronic devices by recognition-based assembly as well as biological sensing.

3.2. FET Biosensors

FETs fabricated with S-SWCNTs ***(1)*** and S-NWs ***(4)*** have shown ultrahigh sensitivity for detecting gas molecules such as NH_3, O_2, and NO_2. The high sensitivity and potential for fabricating high-density sensor array makes the nanoscale FETs very attractive. The same principle can be extended to biosensing, particularly since biomolecules such as DNA and proteins are heavily charged under most conditions. S-SWCNT FETs are more sensitive to the binding of such charged species than chemisorbed gas molecules. However, the wet chemical environment that involves various ions and other biomolecules is much more complicated than the operation for gas sensing. So far no direct measurement of the binding of biomolecules on S-SWCNT FETs in the liquid environment has been successfully demonstrated. Only a recent study by Star et al. ***(34)*** has demonstrated the effectiveness of the device structure for specific biotin-streptavidin binding by measurements in the *dried* condition after incubation and washing. A PEI/PEG polymer coating layer has been employed to avoid nonspecific binding. Biotin molecules were attached to the polymer layer for specific molecular recognition. Biotin-streptavidin binding has been detected by changes in the characteristics of a device. Nonspecific binding was observed in devices without the polymer coating, whereas no binding was found for polymer-coated but not biotinylated devices. Streptavidin, in which the biotin-binding sites were blocked by reaction with excess biotin, produced essentially no change in the characteristics of the biotinylated polymer-coated devices.

Besides the difficulty in obtaining direct measurements in liquids, S-SWCNT FET sensors face the problem that the property of the SWCNTs, whether it is semiconducting or metallic, is not controllable with current synthetic methods. A mixture of CNTs with properties varying in a wide range is produced, which makes systematic studies difficult. NWs of semiconductors such as Si and In_2O_3 do not have this limitation because they are always semiconducting, and the dopant type and concentration can be controlled. As a result, the sensitivity can be tuned in the absence of an external gate.

Fig. 5. **(A)** Schematic of a biotin-modified SiNW in FET device (**left**) and after bound with streptavidin (**right**). **(B)** Plot of conductance vs time for a biotin-modified SiNW, in which region 1 corresponds to buffer solution, region 2 corresponds to addition of 250 n*M* streptavidin, and region 3 corresponds to pure buffer solution. **(C)** Conductance vs time for an unmodified SiNW; regions 1 and 2 are the same as in (B). **(D)** Conductance vs time for a biotin-modified SiNW, in which region 1 corresponds to buffer solution and region 2 to addition of a 250 n*M* streptavidin solution preincubated with 4 eq of d-biotin. **(E)** Conductance vs time for a biotin-modified SiNW, in which region 1 corresponds to buffer solution, region 2 corresponds to addition of 25 p*M* streptavidin, and region 3 corresponds to pure buffer solution. Arrows mark the points when solutions were changed. (Reprinted from **ref. *3*** with permission. Copyright 2001 American Association for the Advancement of Science.)

The functionalization of biorecognition probes to the oxide surface with silane linkers is also much more mature. Cui et al. ***(3)*** successfully demonstrated that boron-doped (p-type) SiNW FETs can be used to create highly sensitive, real-time electrically based sensors for biological and chemical species in buffer solutions. The SiNWs with the native oxide surface modified with

3-aminopropyltriethoxysilane exhibited pH-dependent conductance that was linear over a large dynamic range and could be understood in terms of the change in surface charge during protonation and deprotonation. Biotin-modified SiNWs were used to detect streptavidin down to at least a picomolar concentration range. As shown in **Fig. 5B**, the conductance of biotin-modified SiNWs increased almost instantly to a constant value (from region 1 to region 2) on the addition of 250 n*M* streptavidin in 1 m*M* phosphate buffer (pH 9.0) with 10 m*M* NaCl. This conductance value was maintained after switching to a flow of pure buffer solution (region 3), indicating that a negatively charged species was irreversibly bound to the p-type SiNW surface, consistent with the small dissociation constant ($K_d \sim 10^{-15}$ *M*) for biotin-streptavidin. By contrast, the conductance did not show any change on the addition of (1) the streptavidin solution with an unmodified SiNW (**Fig. 5C**) and (2) a streptavidin solution in which the biotin-binding sites were blocked by reaction with 4 eq of d-biotin with a biotin-modified SiNW (**Fig. 5D**), indicating no nonspecific binding of streptavidin in either case. A similar conductance change resulting from biotin-streptavidin binding was observed when the streptavidin concentration was lowered to 25 p*M* (**Fig. 5E**) with a possible detection limit of about 10 p*M*. In addition, biotin-functionalized SiNWs showed a decrease in conductance on the reversible specific binding of positively charged antibody (monoclonal antibiotin). Concentration-dependent detection was demonstrated in real time down to a concentration of a few nanomolar. Finally, detection of the reversible binding of the metabolic indicator Ca^{2+} was demonstrated using a calmodulin-modified SiNW. The small size, great reliability, and capability of these semiconductor NW FETs for sensitive, label-free, and real-time detection of a wide range of chemical and biological species have great potential for molecular diagnostics.

3.3. Nanoelectrode Array-Based Electrochemical Biosensors

The embedded CNT array minimizes background from the sidewalls while the well-defined graphitic chemistry at the exposed open ends allows the selective functionalization of –COOH groups with primary amine-terminated oligonucleotide probes through amide bonds. The wide electropotential window of carbon makes it possible to measure directly the oxidation signal of guanine bases immobilized at the electrode surface. The probe [Cy3]5'-CTIIAT TTCICAIITCCT-3'[AmC7-Q] and the target [Cy5]5'-AGGACCTGCGAA ATCCAGGGGGGGGGG-3' are used, which are related to the wild-type (Arg1443stop) *BRCA1* gene ***(107)***. A 10-bp polyG is attached to the target sequence as the signal moiety and the guanine bases in the probe are replaced with inosine to ensure that guanine signal is only from target DNA. Hybridization is carried out at 40°C for about 1 h in approx 100 n*M* target solution in

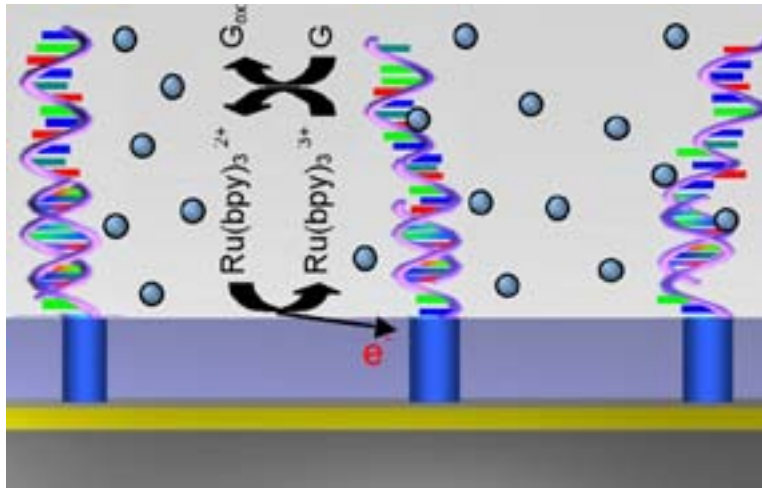

Fig. 6. Schematic of MWCNT nanoelectrode array combined with $Ru(bpy)_3^{2+}$-mediated guanine oxidation for ultrasensitive DNA detection.

X3 saline sodium citrate (SSC) buffer solution. Rigorous washing using X3 SSC, X2 SSC with 0.1% sodium dodecyl sulfate, and X1 SSC, respectively, at 40°C for 15 min after each probe functionalization and target hybridization process are applied to get rid of the nonspecifically bound DNA molecules, which is critical for obtaining reliable electrochemical data.

Such a solid-state nanoelectrode array has great advantages in stability and processing reliability over other electrochemical DNA sensors based on mixed self-assembled monolayers of small organic molecules. The density of a nanoelectrode can be controlled precisely using lithographic techniques, which, in turn, define the number of probe molecules. The detection limit can be optimized by lowering the nanoelectrode density. However, the electrochemical signal is defined by the number of electrons that can be transferred between the electrode and analytes, which is observable only if it is over the level of the background. In particular, guanine oxidation occurs at rather high potential (approx 1.05 V vs saturated calomel electrode [SCE]) at which a high background is produced by carbon oxidation and water electrolysis. This problem can be solved by introducing $Ru(bpy)_3^{2+}$ mediators to amplify the signal based on an electrocatalytic mechanism ***(108)***. Combining the CNT nanoelectrode array with the $Ru(bpy)_3^{2+}$-mediated guanine oxidation method (as schematically shown in **Fig. 6**), Li et al. ***(35)*** demonstrated that the hybridization of less than a few attomoles of oligonucleotide targets can be easily detected with a $20 \times 20\ \mu m^2$ electrode, with orders-of-magnitude improvement in sensitivity compared to previous electrochemically based DNA detections.

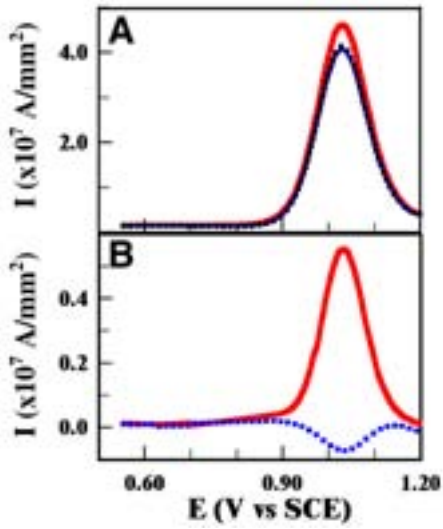

Fig. 7. **(A)** Three consecutive ACV measurements of low-density MWCNT array electrode functionalized with oligonucleotide probes with sequence [Cy3]5'-CTIIAT TTCICAIITCCT-3'[AmC7-Q] and hybridized with oligonucleotide targets with sequence [Cy5]5'-AGGACCTGCGAAATCCAGGGGGGGGGGG-3'. The thick, thin, and dotted lines correspond to the first, second, and third scan, respectively. Measurements were carried out in 5 m*M* $Ru(bpy)_3^{2+}$ in 0.20 *M* NaOAC supporting electrolyte (at pH 4.8) with an AC sinusoidal wave of 10 Hz and 25-mV amplitude on top of a staircase DC ramp. **(B)** Difference between first and second scans (solid line), and between second and third scans (dotted line), respectively. The positive peak corresponds to the increase in $Ru(bpy)_3^{2+}$ oxidation signal owing to the guanine bases on the surface. The negative peak serves as a control representing the behavior of a bare electrode.

Figure 7A shows three consecutive alternating current voltammetry (ACV) scans in 5 m*M* $Ru(bpy)_3^{2+}$ in 0.20 *M* NaOAc buffer solutions after hybridizing the polyG-tagged BRCA1 targets on an MWCNT array electrode (with average tube-tube spacing of approx 1.5 μm). The AC current is measured by applying a sinusoidal wave of 10-Hz frequency and 25-mV amplitude on a staircase potential ramp. Well-defined peaks are observed around 1.04 V, with the first scan clearly higher than the almost superimposed subsequent scans. The background is almost a flat line at zero. As shown in **Fig. 7B**, subtracting the second scan from the first gives a well-defined positive peak (continuous line), whereas subtracting the third scan from the second gives a small negative peak (dashed line) serving as an unambiguous negative control. The high quality of the data indicates that there is still plenty of room to lower the detection limit of target DNAs. In practical diagnosis, the target DNA consists of hun-

dreds of guanine bases as active signal moieties giving a much higher signal. Thus, the detection limit could be reduced well below 1 attomol. Successful electrochemical detection of PCR products using this platform was recently demonstrated. Other advantages of electrochemical detection, such as the ability to apply extra stringency control using an electrical field, could possibly be realized with this system.

The nanoelectrode array platform can also be extended to other electrode materials such as Au and Pt NWs. Different functionalization schemes and signal moieties have to be employed for different applications to take advantage of the spatial and temporal resolution of nanoelectrodes. This platform is also applicable for enzyme-based biosensors or for electrochemically based pathogen detection by immobilizing proteins such as enzymes and antibodies at the electrodes.

3.4. CNT Porous Film Electrodes

Besides being used as building elements in well-defined devices, both SWCNTs and MWCNTs can be cast as a thin film on conventional electrodes ***(78–80)*** or used as a 3D porous film ***(32,36,37)***. CNTs serve both as large immobilization matrices and as mediators to improve electron transfer between the enzyme-active site and the electrochemical transducer. CNT-modified glassy carbon electrodes exhibit a substantial (490 mV) decrease in the overpotential for β-nicotinamide adenine dinucleotide oxidation. Various enzymes such as glucose oxidase and flavin adenine dinucleotide can spontaneously adsorb onto the CNT surface and maintain their substrate-specific enzyme activity over a prolonged period of time ***(78)***. Biosensors based on enzymes that catalyze important biological redox reactions (such as glucose oxidation) can be developed.

3.5. CNT/NW Templated Bioassembly

It is of great interest to modify the external surface of CNTs or NWs with biological macromolecules, such as oligonucleotides ***(109)***, proteins ***(41,94)***, and peptides ***(96)***. Such bio-nanoassembly could promote the development of new biosensors and bioelectronic nanomaterials, which could take advantage of the specific biomolecular recognition properties associated with the bound macromolecules. For such purposes, the specific recognition function has to be densely packed on the outer surface of CNTs/NWs and the biomolecules such as proteins have to remain functional. A good criterion for the conservation of the functional properties of the protein is its ability to form ordered arrays.

Balavoine et al. ***(41)*** reported on a study of streptavidin assembly on CNTs to form helical crystallization. Streptavidin is very useful in many biochemical assays, such as labeling and affinity chromatography, owing to its high affinity

for (+) biotin ($Ka \sim 10^{15}$). The assembly was carried out in solutions by spontaneous adsorption. MWCNTs were prepared by the arc-discharge method and stored as a suspension in methanol (approx 2 mg/mL). One hundred microliters of MWCNT suspension was dried under an ethane gas flow and resuspended in 20 mL of a 40% aqueous solution of methanol. This suspension was sonicated to disperse the MWCNTs prior to the addition of 20 µL of streptavidin solution (approx 10 µg/mL) in a buffer containing 10 m*M* Tris (pH 8.0) and 50 m*M* NaCl, and then it was allowed to stand at room temperature for 45 min. Such a sample was deposited on a carbon film–covered grid and was negatively stained with a 2% uranyl acetate solution for TEM imaging. In appropriate conditions, the MWCNT surface was found almost completely covered with streptavidin, presumably owing to the interaction with its hydrophobic domains. Even though most assemblies are disordered, some regular-spaced helical structures were observed at proper conditions. Another water-soluble protein, HupR, was also studied and showed ordered arrays on a wider range of MWCNT diameters than streptavidin.

A 29-residue amphiphilic α-helical peptide was also specifically designed to coat and solubilize CNTs as well as control the assembly of the peptide-coated CNTs into macromolecular structures through peptide–peptide interactions ***(96)***. **Figure 8** shows a cross-sectional view of the molecular structure and a perspective view of the helical backbones of the model illustrating the assembly of such molecules on an SWCNT surface. Six such α-helices are sufficient to surround the circumference of an individual SWCNT, while maintaining typical interhelical interactions. The hydrophobic face of the helix with apolar amino acid side chains (Val and Phe) presumably interacts noncovalently with the aromatic surface of CNTs, and the hydrophilic face extends outward to promote self-assembly through charged peptide–peptide interactions. Electron microscopy and polarized Raman studies reveal that the peptide-coated CNTs assemble into fibers with CNTs aligned along the fiber axis. The size and morphology of the fibers can be controlled by manipulating solution conditions that affect peptide–peptide interactions.

While the aforementioned studies are based on nonspecific adsorptions, Wang et al. ***(98)*** have used phage display to identify peptides with selective affinity for CNTs. Binding specificity has been confirmed by demonstrating direct attachment of nanotubes to phage and free peptides immobilized on microspheres. Consensus binding sequences show a motif rich in histidine and tryptophan at specific locations. Analysis of peptide conformations shows that the binding sequence is flexible and folds into a structure matching the geometry of CNTs. The hydrophobic structure of the peptide chains suggests that they act as symmetric detergents. An IgG monoclonal antibody against the fullerene C_{60} ***(110)*** was also studied to show binding to CNTs with some selectivity ***(111)***.

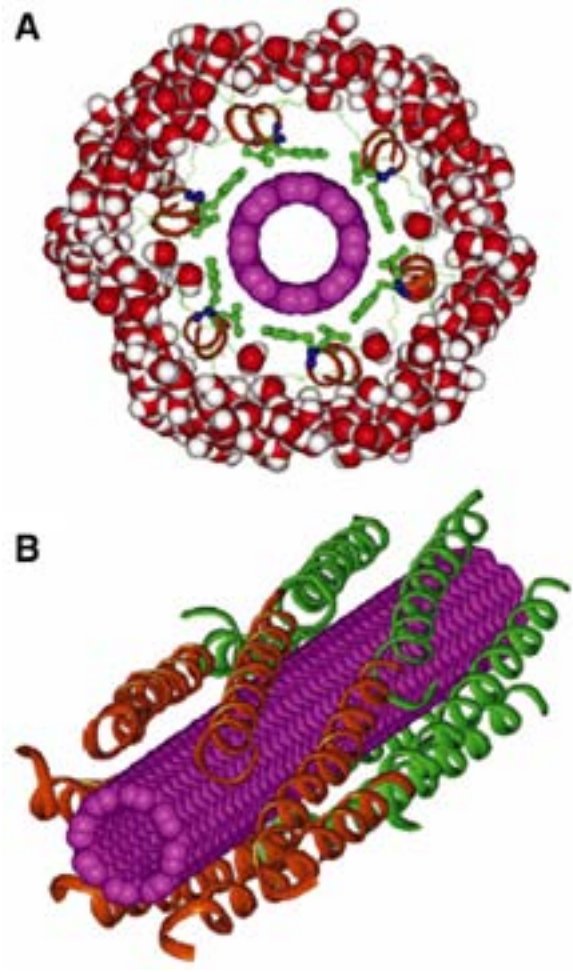

Fig. 8. Model of amphiphilic peptide helices assembled on an SWCNT surface. **(A)** Cross-section view showing six peptide helices wrapped around an SWCNT. A helical ribbon denotes the backbone of each peptide. The hydrophobic Val and Phe side chains are packed against the SWCNT surface. A 5-Å-thick water shell was used in the energy refinement. **(B)** View of a peptide-wrapped SWCNT with 12 peptide helices. The peptide formed two layers with head-to-tail alignment. (Reprinted from **ref. *96*** with permission. Copyright 2003 American Chemical Society.)

3.6. Biomolecular Templated NW Assembly

The steady trend in the electronics industry toward components having ever-smaller dimensions has stimulated the development of alternative "bottom-up" fabrication technologies to compete with conventional micro- and nano-

lithography, which are expected to become extremely expensive as the feature sizes of future electronic circuits approach the limits of optical lithography ***(112)***. Bottom-up approaches, which rely on self-assembly (or self-organization) that often utilizes biological molecules, could provide viable solutions. Low fabrication costs and feature sizes below the current limit of optical lithography are two of the major advantages of bottom-up approaches. Biomolecules can also be employed as templates to deposit various solid materials to form nonhomogeneous NWs, which could possibly be used in electronics-based biosensors.

The chemical deposition of metals such as silver ***(42)***, gold ***(113)***, platinum ***(114,115)***, palladium ***(116,117)***, copper ***(118)***, and functionalized gold particles ***(119,120)*** on DNA has been investigated as a potential approach for creating conductive NWs. The molecular recognition properties of biomolecules are used for the defined buildup of a nanostructured circuit, and the electrical functionality is installed by the directed construction of a metallic wire on the biotemplate. Saxl ***(112)*** and Keren et al. ***(113)*** demonstrated that not only can conducting gold and silver NWs be constructed from DNA templates but also that specific regions of DNA molecules can be protected from metal deposition by associating proteins along sections of the DNA. The ability to control metallization spatially provides an important step toward the bottom-up assembly of functional nanocircuits. However, a nonconducting gap was sometimes observed at small bias voltages. Richter et al. ***(117)*** reported that palladium NWs chemically deposited on a DNA template showed highly conductive ohmic transport behavior. **Figure 9** shows low-voltage (1 kV) SEM images of a single palladium metallized DNA strand with a length of approx 16 μm corresponding to the length of a linear λ-DNA molecule of 48,502 bp. The DNA molecule was positioned between macroscopic Au electrodes and metallized afterward with a two-step chemical deposition method, involving (1) activation of the template by treatment with Pd(II) complexes, which in part bind on the DNA strands, and (2) subsequent reduction of the complexes to form metallic clusters. Two-terminal I-V curves of such NWs showed a linear curve with a bias voltage down to 1 μV ***(117)***. The specific conductivity for NWs with a diameter >50 nm was found only one order of magnitude below that of bulk palladium.

Recently, specific sequences of peptides were used to mineralize specific metals and semiconductors to produce highly crystalline nanocrystals that form nonhomogeneous NW assemblies. A good example is a new biological approach developed by Djalali et al. ***(121)*** to fabricate Au NWs using sequenced histidine-rich peptides as templates. Histidine-containing peptides are known to have high affinities to metal ions that damage central nervous systems by altering protein conformations into abnormal forms via histidine-

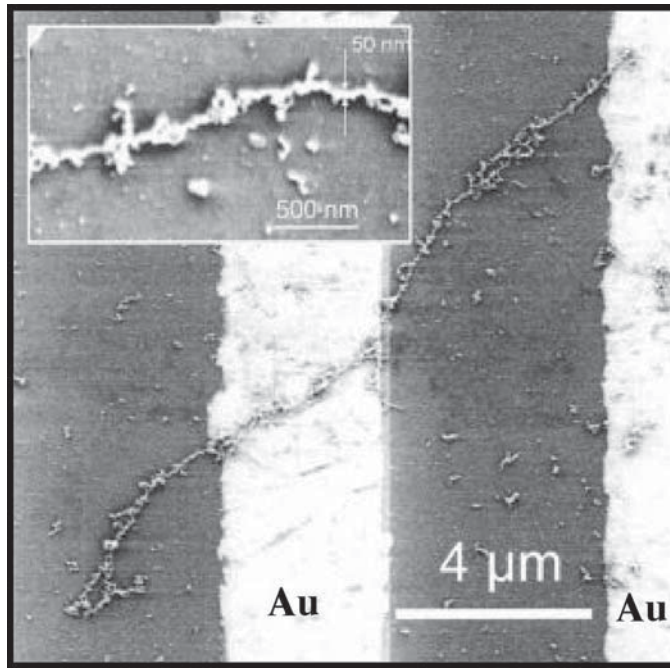

Fig. 9. SEM image of a single palladium metallized DNA strand with length of approx 16 µm corresponding to length of a λ-DNA molecule. Two gold electrodes are deposited on the strands to measure the electrical property across the strand. The inset shows a magnification of the middle part with a diameter of 50 nm. (Reprinted from **ref. *117*** with permission. Copyright 2001 American Institute of Physics.)

metal complexation, and this protein deformation may cause Parkinson disease and Alzheimer disease. Fabrication of the histidine-rich peptide involved four steps. First, *bis*(*N*-α-amido-glycylglycine)-1,7-heptane dicarboxylate molecules (10 m*M*) were self-assembled into NWs in a pH 5.5 citric acid/NaOH solution. Such NWs incorporate binding sites that have high affinity to biological molecules such as DNAs and proteins. Second, a histidine-rich peptide with the sequence A-H-H-A-H-H-A-A-D was immobilized on the heptane dicarboxylate NWs at the binding sites. Third, the histidine-rich peptide NWs were mixed with a $ClAuPMe_3$ solution and incubated for 5 d to allow complete immobilization of Au ions. Finally, a reducing agent, $NaBH_4$, was added to produce Au nanocrystals. By using this method, monodispersed Au nanocrystals were uniformly coated on the histidine peptide NWs with high-density coverage, and the crystalline phases of the Au nanocrystals were observed with TEM.

4. Conclusion

We have summarized recent progress in the development of biological sensors based on CNTs and NWs. The potential of these nanodevices for ultrasensitive biological sensing has been demonstrated from a technology development point of view. The reduction in the size of sensing and transducing elements approaching the size of biomolecules (i.e., 1–100 nm) makes it possible for detection down to single molecules. The development in this field may revolutionize current biotechnologies. However, while the sensitivity improves, the reliability may pose a problem, particularly at the level that only a handful of molecules are to be detected out from the sample containing many other molecules. Extensive efforts must be made in both device fabrication and assay development to solve this issue before the great potential and practical applications can be realized.

Acknowledgments

We wish to thank Drs. M. Meyyappan, Jie Han, Alan Cassell, Wendy Fan, and Harry Partridge for encouragement and technical discussions during preparation of the manuscript. This work was supported by a NASA contract.

References

1 Kong, J., Franklin, N. R., Zhou, C. W., Chapline, M. G., Peng, S., Cho, K., and Dai, H. (2000) Nanotube molecular wires as chemical sensors. *Science* **287,** 622–625.
2. Li, J. and Ng, H. T. (2004) Carbon nanotube sensors, in *Encyclopedia of Nanoscience and Nanotechnology* (Nalwa, H. S., ed.), American Scientific Publishers, Santa Barbara, CA, Vol. 1, 591–601.
3. Cui, Y., Wei, Q., Park, H., and Lieber, C. M. (2001) Nanowire nanosensors for highly sensitive and selective detection of biological and chemical species. *Science* **293,** 1289–1292.
4. Li, C., Zhang D., Liu X., Han, S., Tang, T., Han, J., and Zhou C. (2003) In2O3 nanowires as chemical sensors. *Appl. Phys. Lett.* **82(10),** 1613–1615.
5. Dresselhaus, M. S., Dresselhaus, G., and Eklund, P. C. (ed.). (1996) *Science of Fullerenes and Carbon Nanotubes*, Academic, New York.
6. Ebbessen, T. W. (1997) *Carbon Nanotubes: Preparation and Properties*, CRC Press, Boca Raton, FL.
7. Saito, R., Dresselhaus, M. S., and Dresselhaus, G. (1998) *Physical Properties of Carbon Nanotubes*, World Scientific, New York.
8. Tománek, D. and Enbody, R. (2000) *Science and Application of Nanotubes*, Kluwer Academic, New York.
9. Iijima, S. (1991) Helical microtubules of graphitic carbon. *Nature* **354,** 56–58.
10. Iijima, S. and Ichihashi, T. (1993) Single-shell carbon nanotubes of 1-nm diameter. *Nature* **363,** 603–605.
11. Dai, H. (2002) Carbon nanotubes: synthesis, integration, and properties. *Acc. Chem. Res.* **35(12),** 1035–1044.

12. Collins, P. G., Arnold, M. S., and Avouris, P. (2001) Engineering carbon nanotubes and nanotube circuits using electrical breakdown. *Science* **292,** 706–709.
13. Tans, S. J., Verschueren, A. R. M., and Dekker, C. (1998) Room-temperature transistor based on a single carbon nanotube. *Nature* **393,** 49–52.
14. Fuhrer, M. S., Nygard, J., Shih, L., et al. (2000) Crossed nanotube junctions. *Science* **288,** 494–497.
15. Zhou, C. W., Kong, J., Yenilmez, E., and Dai, H. (2000) Modulated chemical doping of individual carbon nanotubes. *Science* **290,** 1552–1555.
16. Rueckes, T., Kim, K., Joselevich, E., Tseng, G. Y., Cheung, C. L., and Lieber, C. M. (2000) Carbon nanotube-based nonvolatile random access memory for molecular computing. *Science* **289,** 94–97.
17. Derycke, V., Martel, R., Appenzeller, J., and Avouris, P. (2001) Carbon nanotube inter- and intramolecular logic gates. *Nano Lett.* **1(9),** 453–456.
18. Bachtold, A., Hadley, P., Nakanishi, T., and Dekker, C. (2001) Logic circuits with carbon nanotube transistors. *Science* **294,** 1317–1320.
19. Liu, X. L., Lee, C., Zhou, C. W., and Han, J. (2001) Carbon nanotube field-effect inverters. *Appl. Phys. Lett.* **79(20),** 3329–3331.
20. Rosenblatt, S., Yaish, Y., Park, J., Gore, J., Sazonova, V., and McEuen, P. L. (2002) High performance electrolyte gated carbon nanotube transistors. *Nano Lett.* **2(8),** 869–872.
21. Vigolo, B., Penicaud, A., Coulon, C., Sauder, C., Pailler, R., Journet, C., Bernier, P., and Poulin, P. (2000) Macroscopic fibers and ribbons of oriented carbon nanotubes. *Science* **290,** 1331–1334.
22. de Heer, W. A., Chatelain, A., and Ugarte, D. (1995) A carbon nanotube field-emission electron source. *Science* **270,** 1179, 1180.
23. Rinzler, A. G., Hafner, J. H., Nikolaev, P., Lou, L., Kim, S. G., Tomanek, D., Nordlander, P., Colbert, D. T., and Smalley, R. E. (1995) Unraveling nanotubes: field emission from an atomic wire. *Science* **269,** 1550–1553.
24. Dai, H., Hafner, J. H., Rinzler, A. G., Colbert, D. T., and Smalley, R. E. (1996) Nanotubes as nanoprobes in scanning probe microscopy. *Nature* **384,** 147–150.
25. Wong, S., Joselevich, E., Woolley, A., Cheung, C., and Lieber, C. M. (1998) Covalently functionalized nanotubes as nanometer-sized probes in chemistry and biology. *Nature* **394,** 52–55.
26. Li, J., Cassell, A., and Dai, H. (1999) Carbon nanotubes as AFM tips: measuring DNA molecules at the liquid/solid interfaces. *Surf. Interface Anal.* **28,** 8–11.
27. Nguyen, C. V., Chao, K. J., Stevens, R. M. D., Delzeit, L., Cassell, A., Han, J., and Meyyappan, M. (2001) *Nanotechnology* **12,** 363–367.
28. Liu, C. F., Fan, Y. Y., Liu, M. , Cong, H. T., Chen, H. M., and Dresselhaus, M. S. (1999) Hydrogen storage in single-walled carbon nanotubes at room temperature. *Science* **286,** 1127–1129.
29. Che, G., Lakshmi, B. B., Fisher, E. R., and Martin, C. R. (1998) Carbon nanotubule membranes for electrochemical energy storage and production. *Nature* **393,** 346–349.

30. Collins, P. G., Bradley, K., Ishigami, M., and Zettl, A. (2000) Extreme oxygen sensitivity of electronic properties of carbon nanotubes. *Science* **287,** 1801–1804.
31. Sumanasekera, G. U., Adu, C. K. W., Fang, S., and Eklund, P. C. (2000) Effects of gas adsorption and collisions on electrical transport in single-walled carbon nanotubes. *Phys. Rev. Lett.* **85(5),** 1096–1099.
32. Ng, H. T., Fang, A., Li, J., and Li, S. F. Y. (2001) Flexible carbon nanotube membrane sensory system: a generic platform. *J. Nanosci. Nanotechnol*. **1(4),** 375–379.
33. Besteman, K., Lee, J.-O., Wiertz, F. G. M., Heering, H. A., and Dekker, C. (2003), Enzyme-coated carbon nanotubes as single-molecule biosensors. *Nano Lett.* **3(6),** 727–730.
34. Star, A., Gabriel, J.-C. P., Bradley K., and Gruner, G. (2003), Electronic detection of specific protein binding using nanotube FET devices. *Nano Lett.*, in press.
35. Li, J., Ng, H. T., Cassell, A., Fan, W., Chen, H., Ye, Q., Koehne, J., Han, J., and Meyyappan, M. (2003), Carbon nanotube nanoelectrode array for ultrasensitive DNA detection. *Nano Lett.* **3(5),** 597–602.
36. Li, J., Cassell, A., Delzeit, L., Han, J., and Meyyappan, M. (2002) Novel three-dimensional electrodes: electrochemical properties of carbon nanotube ensembles. *J. Phys. Chem. B* **106,** 9299–9305.
37. Sotiropoulou, S. and Chaniotakis, N. A. (2003) Carbon nanotube array-based biosensor. *Anal. Bioanal. Chem.* **375,** 103–105.
38. Walter, E. C., Penner R. M., Liu, H., Ng, K. H., Zach, M. P., and Favier, F. (2002) Sensors from electrodeposited metal nanowires. *Surf. Interface Anal.* **34,** 409–412.
39. Morales, A. M. and Lieber, C. M. (1998) A laser ablation method for the synthesis of crystalline semiconductor nanowires. *Science* **279,** 208–211.
40. Huang, M. H., Mao, S. Feick, H., Yan, H., Wu, Y., Kind, H., Weber, E., Russo, R., and Yang, P. (2001) Room-temperature ultraviolet nanowires nanolasers. *Science* **292,** 1897–1899.
41. Balavoine, F., Schultz, P., Richard, C., Mallouh, V., Ebbesen, T. W., and Mioskowski, C. (1999) Helical crystallization of proteins on carbon nanotubes: a first step towards the development of new biosensors. *Angew. Chem. Int. Ed.* **38(13/14),** 1912–1915.
42. Braun, E., Eichen, Y., Sivan, U., and Ben-Yoseph, G. (1998) DNA-templated assembly and electrode attachment of a conducting silver wire. *Nature* **391,** 775–778.
43. Bethune, D. S., Kiang, C. H., de Vries, M. S., Gorman, G., Savoy, R., Vazquez, J., and Beyers, R. (1993) Cobalt-catalyzed growth of carbon nanotubes with single-atomic-layer walls. *Nature* **363,** 605–607.
44. Thess, A., Lee, R., Nikolaev, P., et al. (1996) Crystalline ropes of metallic carbon nanotubes. *Science* **273,** 483–487.
45. Kajiura, H., Tsutsui, S., Huang, H., Miyakoshi, M., Hirano, Y., Yamada, A., and Ata, M. (2001) Production of single-walled carbon nanotube ropes under controlled gas flow conditions. *Chem. Phys. Lett.* **346,** 356–360.

46. Journet, C., Maser, W., Bernier, P., Loiseau, A., Delachapelle, M., Lefrant, S., Deniard, P., Lee, R., and Fischer, J. (1997) Large-scale production of single-walled carbon nanotubes by the electric-arc technique. *Nature* **388,** 756–758.
47. Kong, J., Cassell, A. M., and Dai, H. (1998) Chemical vapor deposition of methane for single-walled carbon nanotubes. *Chem. Phys. Lett*. **292,** 567–574.
48. Su, M., Zheng, B., and Liu, J. (2000) A scalable CVD method for the synthesis of single-walled carbon nanotubes with high catalyst productivity. *Chem. Phys. Lett*. **322,** 321–326.
49. Colomer, J.-F., Stephan, C., Lefrant, S., Tendeloo, G., Willems, I., Kónya, Z., Fonseca, A., Laurent, C., and Nagy, J. (2000) Large-scale synthesis of single-wall carbon nanotubes by catalytic chemical vapor deposition (CCVD) method. *Chem. Phys. Lett*. **317,** 83–89.
50. Flahaut, E., Govingaraj, A., Peigney, A., Laurent, C., and Rao, C. N. R. (1999) Synthesis of single-walled carbon nanotubes using binary (Fe, Co, Ni) alloy nanoparticles prepared in situ by the reduction of oxide solid solutions. *Chem. Phys. Lett*. **300,** 236–242.
51. Hafner, J., Bronikowski, M., Azamian, B., Nikolaev, P., Colbert, D., and Smalley, R. E. (1998) Catalytic growth of single-wall carbon nanotubes from metal particles. *Chem. Phys. Lett*. **296,** 195–202.
52. Bronikowski, M. J., Willis, P. A., Colbert, D. T., Smith, K. A., and Smalley, R. E. (2001) Gas-phase production of carbon single-walled nanotubes from carbon monoxide via the HiPco process: a parametric study. *J. Vac. Sci. Technol. A* **19,** 1800–1805.
53. Ren, Z. F., Huang, Z. P., Xu, J. W., Wang, J. H., Bush, P., Siegal, M. P., and Provencio, P. N. (1998) Synthesis of large arrays of well-aligned carbon nanotubes on glass. *Science* **282,** 1105–1107.
54. Delzeit, L., McAninch, I., Cruden, B. A., Hash, D., Chen, B., Han, J., and Meyyappan, M. (2002) Growth of multiwall carbon nanotubes in an inductively coupled plasma reactor. *J. Appl. Phys.* **91,** 6027–6033.
55. Li, J., Ye, Q., Cassell, A., Ng, H. T., Stevens, R., Han, J., and Meyyappan, M. (2003) Bottom-up approach for carbon nanotube interconnects. *Appl. Phys. Lett.* **82(15),** 2491–2493.
56. Stejny, J. J. Trinder, R. W., and Dlugosz, J. (1981) Preparation and structure of poly(sulphur nitride) whiskers. *J. Mater. Sci*. **16,** 3161–3170.
57. Golden, J. H., DiSalvo, F. J., Frecht, J. M. J., Silcox, J., Thomas, M., and Elman, J. (1996) Subnanometer-diameter wires isolated in a polymer matrix by fast polymerization. *Science* **273,** 782–785.
58. Venkataraman, L. and Lieber, C. M. (1999) Molybdenum selenide molecular wires as one-dimensional conductors. *Phys. Rev. Lett.* **83,** 5334–5337.
59. Gates, B., Mayers, B., Cattle, B., and Xia, Y. (2002) Synthesis and characterization of uniform nanowires of trigonal selenium. *Adv. Funct. Mater*. **12,** 219–227.
60. Limmer, S. J. Seraji, S., Wu, Y., Chou, T. P., Nguyen, C., and Cao, G. (2002) Template-based growth of various oxide nanorods by sol-gel electrophoresis. *Adv. Funct. Mater.* **12,** 59–64.

61. Barbic, M., Mock, J. J., Smith, D. R., and Schultz, S. (2002) Single crystal silver nanowires prepared by the metal amplification method. *J. Appl. Phys*. **91,** 9341–9345.
62. Molares, M. E. T., Buschmann, V., Dobrev, D., Neumann, R., Scholz, R., Schuchert, I. U., and Vetter, J. (2001) Single-crystalline copper nanowires produced by electrochemical deposition in polymeric ion track membranes. *Adv. Mater.* **13,** 62–65.
63. Müller, T., Heinig, K.-H., and Schmidt, B. (2001) Formation of Ge nanowires in oxidized silicon V-grooves by ion beam synthesis. *Nucl. Instrum. Methods Phys. Res.* **175,** 468–473.
64. Sugawara, A., Coyle, T., Hembree, G. G., and Scheinfein, M. R. (1997) Self-organized Fe nanowire arrays prepared by shadow deposition on NaCl(110) templates. *Appl. Phys. Lett.* **70,** 1043–1045.
65. Xia, Y., Yang, P. Sun, Y., Wu, Y., Mayers, B., Gates, B., Yin, Y., Kim, F., and Yan, H. (2003) One-dimensional nanostructures: synthesis, characterization, and applications. *Adv. Mater.* **15,** 353–389.
66. Zhang, Y., Wang, N., Gao, S., He, R.,Maio, S., Liu, J., Zhu, J., and Zhang, X. (2002) A simple method to synthesize nanowires. *Chem. Mater.* **14,** 3564–3568.
67. Yang, P. and Lieber, C. M. (1997) Nanostructured high-temperature superconductors: creation of strong-pinning columnar defects in nanorod/superconductor composites. *J. Mater. Res.* **12,** 2981–2996.
68. Shi, W.-S., Peng, H.-Y., Zheng, Y.-F., Wang, N., Shang, N.-G., Pan, Z.-W., Lee, C.-S., and Lee, S.-T. (2000) Synthesis of large areas of highly oriented, very long silicon nanowires. *Adv. Mater.* **12,** 1343–1345.
69. Duan, X. F. and Lieber, C. M. (2000) General synthesis of compound semiconductor nanowires. *Adv. Mater.* **12,** 298–302.
70. Wu, Y. and Yang, P. (2000) Germanium nanowire growth via simple vapor transport. *Chem. Mater*. **12,** 605–607.
71. Chen, C. C., Yeh, C. C., Chen, C. H., Yu, M. Y., Liu, H. L., Wu, J. J., Chen, K. H., Chen, L. C., Peng, J. Y., and Chen, Y. F. (2001) Catalytic growth and characterization of gallium nitride nanowires. *J. Am. Chem. Soc*. **123,** 2791–2798.
72. Wang, Y. W., Zhang, L. D., Liang, C. H., Wang, G. Z., and Peng, X. S. (2002) Catalytic growth and photoluminescence properties of semiconductor single-crystal ZnS nanowires. *Chem. Phys. Lett.* **357,** 314–318.
73. Huang, M. H., Feick, H., Webber, E., and Yang, P. (2001) Catalytic growth of zinc oxide nanowires through vapor transport. *Adv. Mater.* **13,** 113–116.
74. Vo-Dinh, T., Alarie, J.-P., Cullum, B. M., and Griffin, G. D. (2000) Antibody-based nanoprobe for measurement of a fluorescent analyte in a single cell. *Nat. Biotechnol.* **18,** 764–767.
75. Campbell, J. K., Sun, L., and Crooks, R. M. (1999) Electrochemistry using single carbon nanotubes. *J. Am. Chem. Soc.* **121,** 3779–3780.
76. Bard, A. J. (1994) *Integrated Chemical Systems: A Chemical Approach to Nanotechnology*, John Wiley & Sons, New York, pp. 27–33.

77. Zhao, J., Buldum, A., Han, J., and Lu, J. P. (2002) Gas molecule adsorption in carbon nanotubes and nanotube bundles. *Nanotechnology* **13,** 195–200.
78. Guiseppi-Elie, A., Lei, C., and Baughman, R. H. (2002) Direct electron transfer of glucose oxidase on carbon nanotubes. *Nanotechnology* **13,** 559–564.
79. Azamian, B. R., Davis, J. J., Coleman, K. S., Bagshaw, C. B., and Green, M. L. H. (2002) Bioelectrochemical single-walled carbon nanotubes. *J. Am. Chem. Soc.* **124,** 12,664, 12,665.
80. Musameh, M., Wang, J., Merkoci, A., and Lin, Y. (2002) Low-potential stable NADH detection at carbon-nanotube-modified glassy carbon electrodes. *Electrochem. Commun.* **4,** 743–746.
81. Kuhr, W. G. (2000) Electrochemical DNA analysis comes of age. *Nat. Biotechnol.* **18,** 1042, 1043.
82. Sosnowski, R. G., Tu, E., Butler, W. F., O'Connell, J. P., and Heller, M. J. (1997) Rapid determination of single base mismatch mutations in DNA hybrids by direct electric field control. *Proc. Natl. Acad. Sci. USA* **94,** 1119–1123.
83. Umek R. M., Lin, S. W., Vielmetter, J., et al. (2001) Electronic detection of nucleic acids: a versatile platform for molecular diagnosis. *J. Mol. Diagn.* **3(2),** 74–84.
84. Popovich, N. D. and Thorp H. H. (2002) New strategies for electrochemical nucleic acid detection. *Interface* **11(4),** 30–34.
85. Wightman, R. M. (1981) Microvoltammetric electrodes. *Anal. Chem*. **53,** 1125A–1134A.
86. Penner, R. M., Heben, M. J., Longin, T. L., and Lewis, N. S. (1990) Fabrication and use of nanometer-sized electrodes in electrochemistry. *Science* **250,** 1118–1121.
87. Fan, F.-R. F. and Bard, A. J. (1995) Electrochemical detection of single molecules. *Science* **267**, 871–874.
88. Li, J., Stevens, R., Delzeit, L., Ng, H. T., Cassell, A. M., Han, J., and Meyyappan, M. (2002) Electronic properties of multiwalled carbon nanotubes in an embedded vertical array. *Appl. Phys. Lett*. **81(5),** 910–912.
89. McCreery, R. L. (1991) Carbon electrodes: structural effects on electron transfer kinetics, in *Electroanalytical Chemistry* vol. 17 (Bard, A. J., ed.), Marcel Dekker, New York, pp. 221–374.
90. Nugent, J. M., Santhanam, R. A., and Ajayan, P. M. (2001) Fast electron transfer kinetics on multiwalled carbon nanotube microbundle electrodes. *Nano Lett.* **1(2),** 87–91.
91. Wong, S. S., Woolley, A. T., Joselevich, E., Cheung, C. L., and Lieber, C. M. (1998) Covalent-functionalized single-walled carbon nanotube probe tips for chemical force microscopy. *J. Am. Chem. Soc.* **120,** 8557, 8558.
92. Williams, K. A., Veenhuizen, P. T. M., De la Torre, B. G., Eritja, R., and Dekker, C. (2002) Carbon nanotubes with DNA recognition. *Nature* **429,** 761.
93. Nguyen, C. V., Delzeit, L., Cassell, A. M., Li, J., Han, J., and Meyyappan, M. (2002) Preparation of nucleic acid functionalized carbon nanotube arrays. *Nano Lett.* **2(10),** 1079–1081.

94. Chen, R. J., Zhang, Y., Wang, D., and Dai, H. (2001) Noncovalent sidewall functionalization of single-walled carbon nanotubes for protein immobilization. *J. Am. Chem. Soc.* **123,** 3838, 3839.
95. Shim, M., Kam, N. W. S., Chen, R. J., Li, Y., and Dai, H. (2002) Functionalization of carbon nanotubes for biocompatibility and biomolecular recognition. *Nano Lett.* **2(4),** 285–288.
96. Dieckmann, G. R., Dalton, A. B., Johnson, P. A., et al. (2003) Controlled assembly of carbon nanotubes by designed amphiphilic peptide helices. *J. Am. Chem. Soc*. **125(7),** 1770–1777.
97. Sun, Y.-P., Fu, K., Lin, Y., and Huang, W. (2002) Functionalized carbon nanotubes: properties and applications. *Acc. Chem. Res*. **35,** 1096–1104.
98. Wang, S., Humphreys, E. S., Chung, S. Y., et al. (2003) Peptides with selective affinity for carbon nanotubes. *Nat. Mater*. **2(3),** 196–200.
99. Ulman, A. (1991) *An Introduction to Ultrathin Organic Films: From Langmuir-Blodgett to Self-Assembly*, Academic, New York.
100 Guo, Z., Guilfoyle, R. A., Thiel, A. J., Wang, R., and Smith, L. M. (1994) Direct fluorescence analysis of genetic polymorphisms by hybridization with oligonucleotide arrays on glass supports. *Nucleic Acids Res*. **22(24),** 5456–5465.
101 Beier, M. and Hoheisel, J. D. (1999) Versatile derivatisation of solid support media for covalent bonding on DNA-microchips. *Nucleic Acids Res*. **27(9),** 1970–1977.
102 Vo-Dinh, T. (2002) Nanobiosensors: probing the sanctuary of individual living cells. *J. Cell. Biochem. Suppl.* **39,** 154–161.
103 Vo-Dinh, T., Cullum, B. M., and Stokes, D. L. (2001) Nanosensors and biochips: frontiers in biomolecular diagnostics. *Sens. Actuators B* **74,** 2–11.
104 Johnson, J. C., Yan, H., Schaller, R., Haber, L. H., Saykally, R. J., and Yang, P. (2001) Single nanowires lasers. *J. Phys. Chem. B* **105(46),** 11,387–11,390.
105 Woolley, A. T., Guillemette, C., Cheung, C. L., Housman, D. H., and Lieber, C. M. (2000) Direct haplotyping of kilobase-size DNA using carbon nanotube probes. *Nat. Biotechnol.* **18,** 760–763.
106. Andrew, T. and Mirkin, C. A. (2000) Haplotyping by force. *Nat. Biotechnol.* **18,** 713.
107 Miki, Y., Swensen, J., Shattuck-Eidens, D., Futreal, P. A., Harshman K., Tavtigian, S., Liu, Q., Cochran, C., Bennett, L. M., and Ding, W. (1994) A strong candidate for the breast and ovarian cancer susceptibility gene BRCA1. *Science* **266,** 66–69.
108 Sistare, M. F., Holmberg, R. C., and Thorp, H. H. (1999) Electrochemical studies of polynucleotide binding and oxidation by metal complexes: effects of scan rate, concentration, and sequence. *J. Phys. Chem. B* **103,** 10,718–10,728.
109 Guo, Z., Sadler, P. J., and Tsang, S. C. (2002) Immobilization and visualization of DNA and proteins on carbon nanotubes. *Adv. Mater.* **10(9),** 701–703.
110. Braden, B. C. (2000) X-ray crystal structure of an anti-Buckminsterfullerene antibody Fab fragment: biomolecular recognition of C60. *Proc. Natl. Acad. Sci. USA* **97,** 12,193–12,197.

111. Erlanger, B. F., Chen, B.-X., Zhu, M., and Brus, L. (2001) Binding of an anti-fullerene IgG monoclonal antibody to single wall carbon nanotubes. *Nano Lett.* **1,** 465–467.
112. Saxl, O. (2001) *Opportunities for industry in the application of nanotechnology*. The Institute of Nanotechnology, Stirling, Scotland (http://www.nano.org.uk/contents.htm).
113. Keren, K., Krueger, M., Gilad, R., Ben-Yoseph, G., Sivan, U., and Braun, E. (2002) Sequence-specific molecular lithography on single DNA molecules. *Science* **297,** 72–75.
114. Ford, W., Harnack, O., Yasuda, A., and Wessels, J. M. (2001) Platinated DNA as precursors to templated chains of metal nanoparticles. *J. Adv. Mater*. **13,** 1793–1797.
115. Seidel, R., Mertig, M., and Pompe, W. M. (2002) Scanning force microscopy of DNA metallization. *Surf. Interface Anal*. **33,** 151–154.
116. Richter, J., Seidel, R., Kirsh, R., Mertig, M., Pompe, W., Plaschke, J., and Schackert, H. K. (2000) Nanoscale palladium metallization of DNA. *Adv. Mater*. **12,** 507–510.
117. Richter, J., Mertig, M., Pompe, W., Mönch, I., and Schackert, H. K. (2001) Construction of highly conductive nanowires on a DNA template. *Appl. Phys. Lett*. **78,** 536–538.
118. Christopher, A., Monon, F., and Woolley, A. T. (2003) DNA-templated construction of copper nanowires. *Nano Lett.* **3(3),** 359–363.
119. Harnack, O., Ford, W. E., Yasuda, A., and Wessels, J. M. (2002) Tris(hydroxymethyl)phosphine-capped gold particles templated by DNA as nanowire precursors. *Nano Lett.* **2(9),** 919–923.
120. Patolsky, F., Weizmann, Y., Lioubashevski, O., and Willner, I. (2002) Au-nanoparticle nanowires based on DNA and polylysine templates. *Angew. Chem. Int. Ed.* **41(13),** 2323–2327.
121. Djalali, R., Chen, Y., and Matsui, H. (2002) Au nanowire fabrication from sequenced histidine-rich peptide. *J. Am. Chem. Soc.* **124(46),** 13,660–13,661.